LA-UR-01-3490
Approved for public release;
distribution is unlimited.

Title:

INVESTIGATION OF THE OBSERVED ANISOTROPIC FRACTURE IN STEELS

Author(s):

B. E. Clements and E. M. Mas
(T-1) Theoretical Division, Los Alamos National Laboratory, Los Alamos, NM 87545
G. T. Gray III
(MST-8) Materials Science Division, Los Alamos National Laboratory, Los Alamos, NM 87545

Submitted to:

http://lib-www.lanl.gov/la-pubs/00818473.pdf

INVESTIGATION OF THE OBSERVED ANISOTROPIC FRACTURE IN STEELS

B. E. Clements and E. M. Mas

(T-1) Theoretical Division, Los Alamos National Laboratory, Los Alamos, NM 87545

G. T. Gray III

(MST-8) Materials Science Division, Los Alamos National Laboratory, Los Alamos, NM 87545

Abstract. A theory has been developed to model the fracture of 1080 steels. In the process of hot rolling, high aspect ratio MnS inclusions condense in 1080 steels. The inclusions align along the rolling direction. Even though the volume concentration of these inclusions is low, fractography has shown that they have a substantial effect on the fracture characteristics of the steel. We use the Method of Cells (MOC) to model this system with a (2x2x2) representative volume element to model micro-structural effects. One of the eight MOC cells contains an elongated MnS inclusion while the remaining seven cells contain pure 1080 steel. The steel is modeled using the von Mises plasticity model. Weak interfacial bonding between the MnS and 1080 steel is assumed. We compare MOC with TEPLA to study the void growth characteristics of the MOC theory. Finally, we implement the MOC theory in the finite-element code EPIC, carry out 3-dimensional plate impact experiments, and compare our results with the plate impact experiments of Gray and Bourne.

INTRODUCTION

The fracture properties of 1080 steel is an interesting system to study because of its unusual anisotropic fracture characteristics that are known to arise from low concentrations of manganese sulfide (MnS) impurities. These impurities condense, in the hot rolling process, to form elongated (high aspect ratio) aligned inclusions. The alignment direction coincides with the rolling direction and is the origin of the orientation dependence (the anisotropy) of the fracture.

G. Gray and N. Bourne have carried out plate impact experiments on 1080 steel that demonstrate the anisotropic nature of the fracture[1]. Fgure 1 is the measured longitudinal stress for three plate impact experiments. The two profiles marked Longitudinal and Transverse were obtained from mild steel (E3N low carbon steel) impacting 1080 steel at a velocity of 208 m/s (see Fig. 2). The flyer was 3mm thick and the 1080 target was 6 mm thick in the experiments.

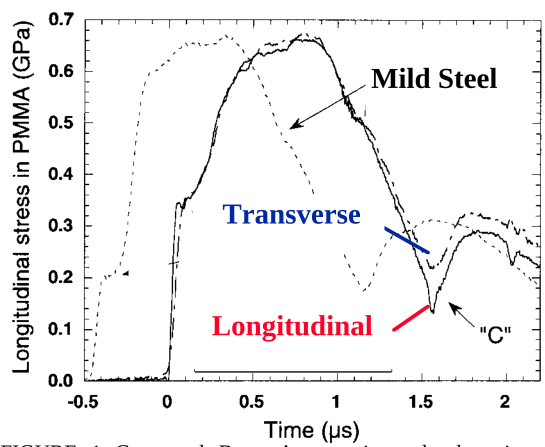

FIGURE 1 Gray and Bourne's experimental plate impact velocity profiles for 1080 steel spall studies.

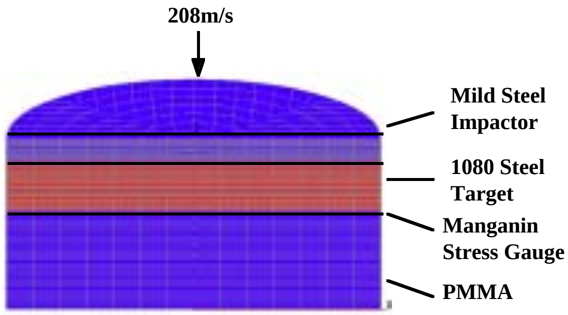

FIGURE 2 Schematic of Gray and Bourne's plate impact experiment for 1080 steel spall studies.

The profile marked mild steel was a symmetric impact experiment. Manganin stress gauges, measuring the longitudinal stress, were fixed to the rear surface of the 1080 steel and were held in place with a PMMA block. The alignment direction of the MnS inclusions was chosen to be either along the direction of the experiment (denoted as longitudinal) or perpendicular to the axial direction of the experiment (denoted as transverse). In these experiments the 1080 steel spalled and the pull back (point C) in the profile occurs at about 2.6 μs after impact. The profiles show a clear distinction between the longitudinal and transverse experiments.

This observation is an experimental indication of anisotropic fracture. Metallographic fractography shows that the MnS plays a significant role in the fracture of 1080 steel. Examination of the spalled 1080 sample shows that the MnS inclusions act as microvoid initiation sites. Consequently, if one is to model this system, and its fracture characteristics, it is of paramount importance to include the orientation and shape of the MnS inclusions.

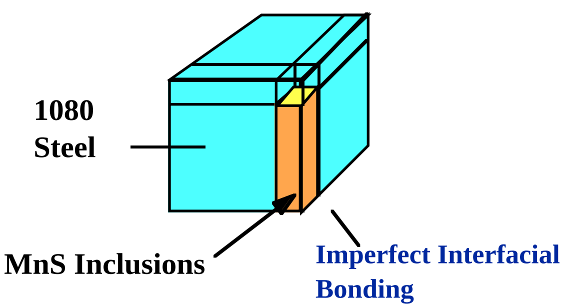

FIGURE 3. The (2x2x2) RVE used in this work to model 1080 steel s using the MOC analysis.

Here we propose a novel way to model the anisotropic fracture of 1080 steel. The Method of Cells (MOC) micro-mechanics model is a convenient method to handle the elongated MnS inclusions and the mechanical properties of the pure 1080 steel. Since the MOC assumes a periodically repeating representative volume element (RVE), the inclusion alignment in this problem is readily taken into account. We use an eight-cell RVE for our model. This so-called (2x2x2) RVE contains one cell with MnS and the seven remaining cells contain pure 1080 steel. While this RVE is the simplest one imaginable that captures some of the details of the real system, it does have some easily recognized deficiencies. For example, the aspect ratios for the inclusions are not constant but range between 1 (spherical) to over 100 (string-like). The lengths of the longer inclusions are over 100 μm. Other impurities also inhabit the 1080 system. In spite of deficiencies we will first model the system with the simple (2x2x2) RVE and defer the extension to more general RVE's for future work.

METHOD OF CELLS

A detailed discussion of the MOC has been given by Aboudi[2]. The MOC equations are derived from the following considerations: (1) volume averaged stress is continuous across cell boundaries, (2) volume averaged displacement is continuous across cell boundaries when interfacial bonding is perfect, (3) a first-order expansion suffices for the local particle displacement field, (4) conditions of mechanical equilibrium apply, (5) constitutive laws for the constituent materials are known, and (6) the micro-structure is spatially periodic (allowing the identification of a RVE). These conditions are sufficient to solve for the micro-stresses $\sigma_{ij}^{(\alpha,\beta,\gamma)}$ and micro-strains $\varepsilon_{ij}^{(\alpha,\beta,\gamma)}$ in the RVE cells. The macro-stress $\overline{\sigma}_{ij}$ for the entire composite system, for example, is determined from the weighted volume average of the micro-stresses

$$\overline{\sigma}_{ij} = \frac{1}{V}\sum_{\alpha,\beta,\gamma} v(\alpha,\beta,\gamma)\,\sigma_{ij}^{(\alpha,\beta,\gamma)}\,, \qquad (1)$$

where V is the total RVE volume, α,β,γ labels the cells of the RVE and $v(\alpha,\beta,\gamma)$ is the volume of the $\alpha,\beta,\gamma^{\text{th}}$ cell.

In Fig. 3 the (2x2x2) RVE used in this work is shown. The single elongated cell represents the MnS inclusion, the remaining cells are pure 1080 steel. Omitting the details, we use von Mises plasticity with Y = 2 Gpa. Longitudinal and shear wave speeds are 5.95 and 3.26 km/s, respectively. EN3 has wave speeds close to these but an approximate yield of 1 Gpa. To handle the volumetric part of the deformation we invoke the Mie-Gruneisen equation of state. HY-100 parameters from the EPIC library[3] were used. There is an interface between the 1080 steel cells and the MnS cell. Because the adhesive strength between these materials is believed to be very weak we make the simplifying assumption that beyond an (arbitrarily) small tensile strain the interface debonds. Thereafter, the region between the expanding 1080 steel and the stationary MnS inclusion is void filled. It is the growth of this interfacial porosity that we will monitor. Upon the system becoming subsequently compressed the interfacial porosity can be squeezed from the system. Once the porosity is reduced to zero the compressive stress must act against the MnS inclusion.

MOC AND TEPLA COMPARISON

Applying the MOC to model void growth appears to be novel, thus it is important to carry out checks on the accuracy of the method. TEPLA[3] is a reliable void growth algorithm, based on Gurson's failure surface for void growth in ductile materials, and provides us with a good model to compare to the MOC void growth model. We used the material constants for TEPLA provided in the EPIC material library for HY-100 steel. The only material parameter that we varied substantially from the library values was the relaxation time constant used in the rate dependent formulation of the theory. The void growth predicted by TEPLA was found to be quite sensitive to the relaxation time chosen.

To compare the MOC and TEPLA predictions, we applied the same tensile boundary condition to both models. An initial (seed) void concentration of 0.001 was chosen. For TEPLA only spherical voids can be modeled while the MOC void was a cube. The system was loaded at a constant tensile rate of

$$\dot{\varepsilon}_{11} = \dot{\varepsilon}_{22} = \dot{\varepsilon}_{33} = 10^4 s^{-1}. \qquad (2)$$

In the MOC, within each HY-100 cell, the plastic strain rate is incompressible, implying

$$\sum_{k=1}^{3} \left[\dot{\varepsilon}_{kk}^{(\alpha\beta\gamma)} \right]^P = 0, \qquad (3)$$

where p denotes the plastic strain rate. Incompressibility of the plastic micro-strain rates was verified numerically. When growing voids are present, the composite plastic strain rate (as determined in the MOC theory) can be computed and is not zero,

$$\sum_{k=1}^{3} \left[\dot{\bar{\varepsilon}}_{kk} \right]^P \equiv \dot{e}_{kk}^{p} \neq 0, \qquad (4)$$

rather, it is proportional to the rate of void growth. Interestingly, this fact is a direct result of the MOC analysis, whereas in TEPLA this fact is added, by hand, as the void growth law.

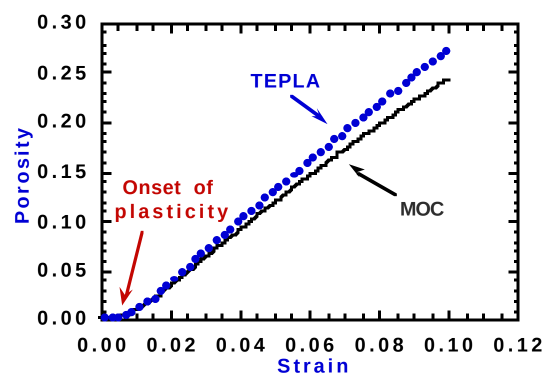

FIGURE 4. Comparison of the MOC and TEPLA void growth analyses. This figure shows the growth of porosity as a function of tensile strain predicted by the two analyses.

Both models used MTS plasticity[3] with identical material parameters. In Fig. 4 the porosity is shown. It is observed that when plasticity is initiated the void growth rapidly increases. The two methods give results in acceptable agreement.

SIMULATIONS OF THE GRAY-BOURNE EXPERIMENT

To model Gray and Bourne's plate impact experiment requires a full three-dimensional simulation. This is because the aligned transverse orientation of the MnS inclusions breaks the two-dimensional cylindrical symmetry often encountered in plate impact geometry. Consequently, we implement the MOC theory into the finite-element code EPIC[3]. All aspects of the theory (plasticity, interfacial debonding, and EOS) have been previously mentioned. The primary difference is that the MnS inclusions are now elongated (aspect ratio = 30) and have either longitudinal or transverse orientations relative to the cylindrical axis of the experiment. Fig. 5 illustrates the two orientations.

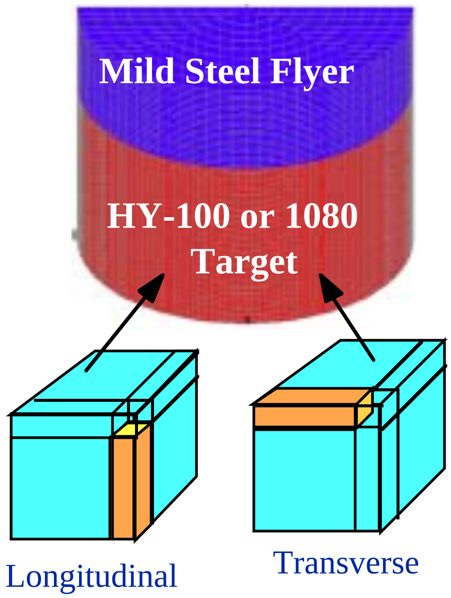

FIGURE 5. An illustration of the two orientations of the MnS inclusions when MOC is implemented in EPIC.

At 2.5 μs after impact a substantial tensile wave is propagating through the 1080 steel. We find that the porosity evolution is quite different for the two orientations. While the transverse orientation produces a smooth porosity profile (similar to that observed for many metals) the longitudinal orientation produces a porosity profile that is highly structured, with patches of the target having insignificant porosity while others have large porosity buildup. This patch-work profile can arise when sudden void growth in a given region acts to relieve the tensile stress in neighboring regions. The result is significantly less void growth occurs in the neighboring regions. We speculate that this phenomena is occurring in 1080 steel.

The velocity profiles determined by EPIC/MOC for the two orientations are shown in Fig. 6. There is a qualitative similarity between these profiles and those of Gray and Bourne (Fig. 1). In our theory the difference in the profiles after 2.5 μs stems from the waves propagating through voided 1080 steel with different porosity distributions. An interfacial spall porosity of 0.29% (Longitudinal) and 0.50% (Transverse) was arbitrarily chosen for the two simulations.

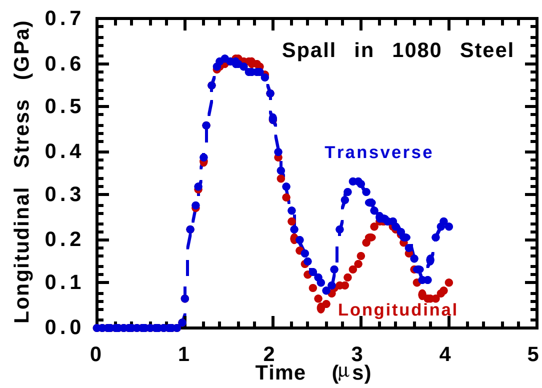

FIGURE 6. Theoretical velocity profile determined from EPIC/MOC.

ACKNOWLEDGMENTS

The authors gratefully acknowledge financial support for this work from the Joint DoD/DOE Munitions Technology Development Program and the (LANL) Laboratory. Research supported by the USDOE under contract W-7405-ENG-36.

REFERENCES

1) G. Gray and N. Bourne (private communication).
2) J. Aboudi, *Mechanics of Composite materials: A Unified Micromechanical Approach*, Elsevier Science Publishers, Amsterdam, 1991.
3) Johnson, G. R., Stryk, R. A., Holmquist, T. J., and Beissel, S. R., *User Instructions for the 1997 Version of the EPIC Code*, Wright Laboratory, Armament Directorate, Eglin Air Force Base report, WL-TR-1997-7037, 1997.